



## Snub boron nanostructures: Chiral fullerenes, nanotubes and planar sheet

Rajendra R. Zope\*, Tunna Baruah

Department of Physics, The University of Texas at El Paso, El Paso, TX 79968, USA

### ARTICLE INFO

#### Article history:

Received 22 September 2010

In final form 3 November 2010

Available online 9 November 2010

### ABSTRACT

We design a new class of electronically stable boron nanostructures, viz.:  $60n^2$  boron fullerene family, boron nanotubes, and a planar boron sheet, which like the  $\alpha$ -boron sheet, consists of triangular and hexagonal motifs and has symmetrically arranged hexagonal holes. The binding energy of the proposed new boron sheet is only 0.02 eV/atom lower than the  $\alpha$ -boron sheet. The  $60n^2$  boron fullerenes are *chiral* and the initial icosahedral symmetry of the fullerenes is lowered due to Jahn–Teller distortion. The smallest *chiral*  $B_{60}$  fullerene is more stable by 1.5 eV than the exact boron analogue of  $C_{60}$  fullerene.

© 2010 Elsevier B.V. All rights reserved.

Carbon has played a dominant role in the field of nanoscience. With the bonding of  $sp^2$  hybridized orbitals carbon can form a variety of different nanostructures such as fullerenes, nanotubes, toroids, nanocones, and flat planar sheet. Though boron has only three valence electrons, it can form  $sp^2$  hybridized orbitals like carbon. The question whether boron can form carbon like hollow nanostructures have piqued interest of several researchers [1–11]. Early works in this direction primarily explored the boron hydrides [12–14]. Subsequent studies examined the stabilities of fullerenes and nanotubes containing buckled triangular motifs [15,16]. A nice summary of these early works can be found in a short review by Quandt and Boustani [17].

In a recent study Swzacki et al. studied a few boron fullerenes in the size range 12–110 atoms and noted a particularly stable highly symmetric  $B_{80}$  fullerene [1]. The structural similarity of the  $B_{80}$  fullerene to that of celebrated  $C_{60}$  fullerene brought this work wide attention. The  $B_{80}$  fullerene can be obtained from  $C_{60}$  fullerene by replacing carbon atoms by boron atoms and by adding 20 extra boron atoms at the centers of 20 hexagons. Swzacki et al. argued that the stability of  $B_{80}$  was due to intertwining of the boron rings (stripes). Later, more elaborate explanation of the stability in terms of chemical bonding was provided by Tang and Ismail-Beigi [8]. They explained the enhanced stability of  $B_{80}$  fullerene as a consequence of its structure which provides an optimal balance of electron rich triangular regions (hexagons with interior boron atom) and electron deficient holes (pentagonal rings). Tang and Ismail-Beigi examined several flat boron sheets and obtained the most stable boron sheet, called  $\alpha$ -boron sheet, which like the  $B_{80}$ , has *evenly-distributed* holes. The  $\alpha$ -boron sheet can be obtained from electron-rich triangular sheet by removing atoms in such a way that the holes (hexagons) are isolated from one another and each

filled hexagon (hexagons with interior boron atom) has three holes and three filled hexagons as nearest neighbors arranged in an alternate fashion. Such an arrangement results in symmetric distribution of holes isolated from each other. Tang and Ismail-Beigi used the hole density,  $\eta$  (defined as the ratio of missing boron atoms to the total number of boron atoms if the sheet were made from a triangular lattice) as a measure of stability of boron sheets. By computing the binding energy of the boron sheets as function of  $\eta$  they found that the stability of boron sheets is maximum around  $\eta = 1/9$ . The most stable  $\alpha$ -boron sheet has hole density of  $1/9$ . The holes in the  $B_{80}$  fullerene are the pentagons. Though  $\eta$  for the  $B_{80}$  is  $12/92$ , its structure is perfectly compatible with the  $\alpha$ -boron sheet which is designed on the idea of balancing electron-rich and electron-deficient regions. Subsequent studies showed that an infinite family of the  $80n^2$  icosahedral boron fullerenes compatible with the  $\alpha$ -boron sheet can be constructed [18]. Such icosahedral fullerenes and other low symmetry fullerenes are more stable than the  $B_{80}$  fullerene [18–20]. These studies have also revealed the similarity in the valence electronic structure of nonmetallic  $\alpha$ -boron fullerenes [9,18] and their parent carbon fullerenes, which results in interesting relation between static polarizabilities of  $\alpha$ -boron and related carbon fullerenes [21].

Boron fullerenes studied so far can be broadly classified into four different types: (i) exact analogue of carbon fullerenes, that is, boron fullerenes obtained by replacing carbon atoms by boron atoms, (ii) boron fullerenes obtained from carbon fullerenes, by replacing carbon atoms by boron atoms and by adding one boron atom to each hexagonal and pentagonal rings [15,16]. These are consistent with Boustani's Aufbau postulate [17] for construction of stable boron structures using hexagonal and pentagonal pyramids. (iii) Boron fullerenes containing hexagonal rings with additional boron atoms at their center and hollow pentagonal holes [17]. (iv)  $\alpha$ -Boron fullerenes compatible with the  $\alpha$ -boron sheet. A very recent study by Ozdoan et al. [22] and Mukhopadhyay et al. [23] illustrated a boron fullerene different from above four

\* Corresponding author.

E-mail address: [rzope@utep.edu](mailto:rzope@utep.edu) (R.R. Zope).

types. This  $B_{100}$  fullerene is 72 meV more stable than the  $\alpha$ - $B_{80}$  fullerene; the corresponding precursor boron sheet has parallel holes each characterized by surrounding six atoms [22]. Most earlier works have studied boron fullerenes of the first three types. The special  $B_{80}$  fullerene with enhanced stability was found by Swazcki et al. while studying boron fullerenes of types ii and iii. The  $B_{80}$  fullerene is the smallest fullerenes of the  $\alpha$ -boron fullerenes (type iv). Boron fullerenes smaller than  $B_{80}$  studied so far are of the first three types. In this Letter, we present, a new structure of the  $B_{60}$  fullerene, which like the  $B_{80}$ , has pentagonal holes (electron deficient regions) isolated from each other by (electron rich) boron stripes in a symmetric fashion. This new  $B_{60}$  fullerene is a chiral distorted snub dodecahedron and is energetically as well as vibrationally stable ( $C_1$  symmetry). It is 0.7 eV more stable than the distorted truncated  $B_{60}$  icosahedron. We further illustrate that new  $B_{60}$  fullerene is the smallest of an infinite class of chiral boron fullerenes. This new family of  $60n^2$  boron fullerenes has initial icosahedral symmetry with each boron atom in fivefold coordination. Density functional calculations on the first three members of this family show that the icosahedral symmetry is lowered due to Jahn–Teller effects and that these boron fullerenes are energetically stable with systematic increase in binding energies with increase in fullerene size. In the infinite limit, these structures become a flat sheet. The structure of the new flat boron sheet, which is different from previously considered boron sheets by Lau and Pandey [24], has (like in the  $\alpha$ -boron sheet) *evenly-distributed* hexagonal holes isolated from each other by triangular zigzag stripes. It can be constructed from the hexagonal sheet using *snub* operation [25]. The binding energy of the new boron sheet is only 0.02 eV/atom lower than the  $\alpha$ -boron sheet. Hereafter, we will refer to this class of boron nanostructures as *snub* boron nanostructures since in the infinite limit, the flat boron sheet has *snub* hexagonal tiling. The snub planar sheet and the fullerenes are described in more detail later.

Our calculations on the boron fullerenes are performed within density functional theory using the NRLMOL code [26–28] and the Vienna ab initio software package (VASP) [29,30]. The former uses a linear combination of Gaussian functions. A large polarized basis set containing 35 basis functions per atom is used [31]. The structure optimization is performed until the forces on all atoms were less than 0.01 eV/Å. The calculations on the periodic boron sheets (and nanotube) are performed using VASP [29,30]. The kinetic energy cut off for the plane wave basis set was chosen as 398 eV. The Brillouin zone was sampled using  $16 \times 16 \times 1$   $\mathbf{k}$  mesh and the projected augmented wave pseudopotentials were used. The structural stability of the  $B_{60}$  and the snub boron sheet was checked by performing vibrational calculations. The Perdew–Burke–Ernzerhof generalized gradient approximation is used to describe the exchange–correlation effects.

The structure of the  $B_{60}$  fullerene is shown in Figure 1. The structure shown on top half of Figure 1 is optimized within the icosahedral symmetry constraint. This icosahedral *snub*  $B_{60}$  fullerene is more stable than the exact the boron analogue of the icosahedral  $C_{60}$  fullerene by 1.5 eV. However, both of these  $B_{60}$  fullerenes have half filled fourfold degenerate highest occupied molecular orbital (HOMO). Jahn–Teller distortion lowers the symmetry to  $C_2$  resulting in the structure on bottom half of Figure 1. The  $C_2$  structure is lower in energy by 0.02 eV and has a wider energy gap of 0.85 eV between the HOMO and the lowest unoccupied molecular orbital (LUMO). Both the icosahedral and the  $C_2$  structures are chiral, that is, their mirror images are not identical to themselves.

Each boron atom in the  $B_{60}$  fullerenes is in fivefold coordination. The 12 pentagons in  $B_{60}$  are separated from each other by a network of 80 triangles. Following Tang and Ismail-Beigi, we explored the idea of using the hole density  $\eta$  as a measure of stability for boron fullerenes. The hole density,  $\eta$ , of the  $B_{60}$  is  $1/6$ , greater than

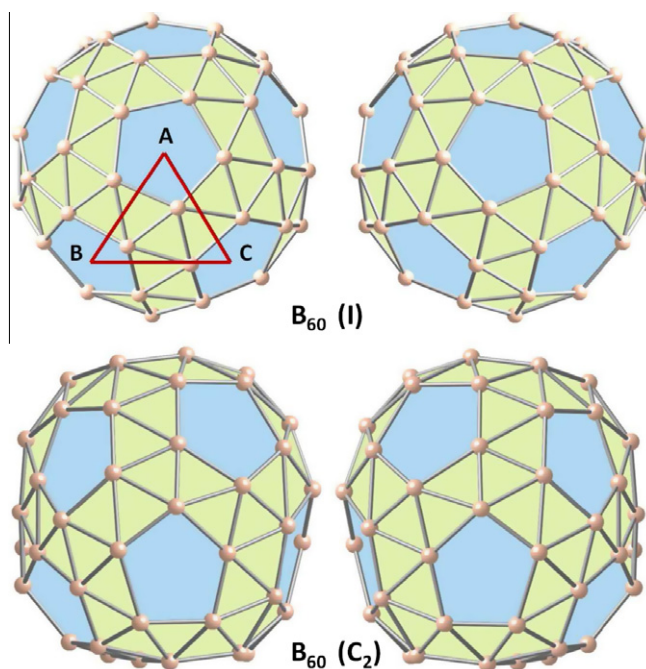


**Figure 1.** The  $B_{60}$  fullerene: perfect icosahedral structure (top) and fully relaxed  $C_2$  structure (bottom). The structures on the right are the mirror images of the structure on the left. The mirror images show the chirality of the structures.

$12/92$  in the  $B_{80}$  fullerene. To examine the effect of reducing hole density towards  $\eta$  of  $B_{80}$  fullerene, we filled some of the pentagonal holes in the  $B_{60}$  clusters to realize the  $B_{61}$ ,  $B_{62}$ ,  $B_{63}$ ,  $B_{64}$  fullerenes. The boron atoms can be added to the pentagonal rings in a number of different ways. We have optimized the structures and studied energetics of all such possible combinations for a given size. Addition of boron atom results in increase in binding energy (calculated using VASP) from 5.5 eV/atom in  $B_{60}$  to 5.57 eV/atom in  $B_{61}$ . The addition of further boron atoms reduces the hole density but does not necessarily lead to significantly higher binding energy. We also optimized the  $B_{72}$  fullerene in which 12 boron atoms cap the 12 pentagonal faces of  $B_{60}$  resulting in zero hole density. The binding energy of the  $B_{72}$  fullerene (with no holes) is essentially same as the parent  $B_{60}$  fullerene. This may appear unusual as the binding energy of a cluster in general increases with increase in the cluster size. When hollow pentagonal rings of  $B_{60}$  are capped with additional boron atoms, the hole density of the fullerene decreases. The  $B_{72}$  fullerene with no holes has the same structural pattern as fullerenes made from triangular lattice. The insignificant difference in the binding energies of  $B_{60}$  and  $B_{72}$  is consistent with observation that boron sheets with hole density around  $1/7$ – $1/9$  are more stable than the triangular sheets [8]. In a recent work on  $\alpha$ -boron fullerenes, we have illustrated a procedure to build  $80n^2$  boron fullerenes from the  $\alpha$ -boron sheet [18]. The planar boron sheet compatible with  $B_{60}$  fullerene can be generated using a similar procedure but in a reverse fashion. The equivalent of the triangle ABC on the  $B_{60}$  fullerene in Figure 1 is shown in Figure 2. The holes in the planar boron sheet will be hexagons as pentagonal rings introduce curvature in the otherwise planar sheet. One can generate a piece of flat boron sheet using  $C_6$  symmetry with the symmetry axis perpendicular to the plane of triangle and passing through one of the apices. If one chooses apex A then the atoms PQRSTU (Figure 2) define a structure unit. The planar boron sheet can be obtained from these structural units and ensuring the compatibility with  $B_{60}$  fullerene. The resultant boron sheet is shown in Figure 2. Such tiling of a plane is called *snub* hexatiles. The structure

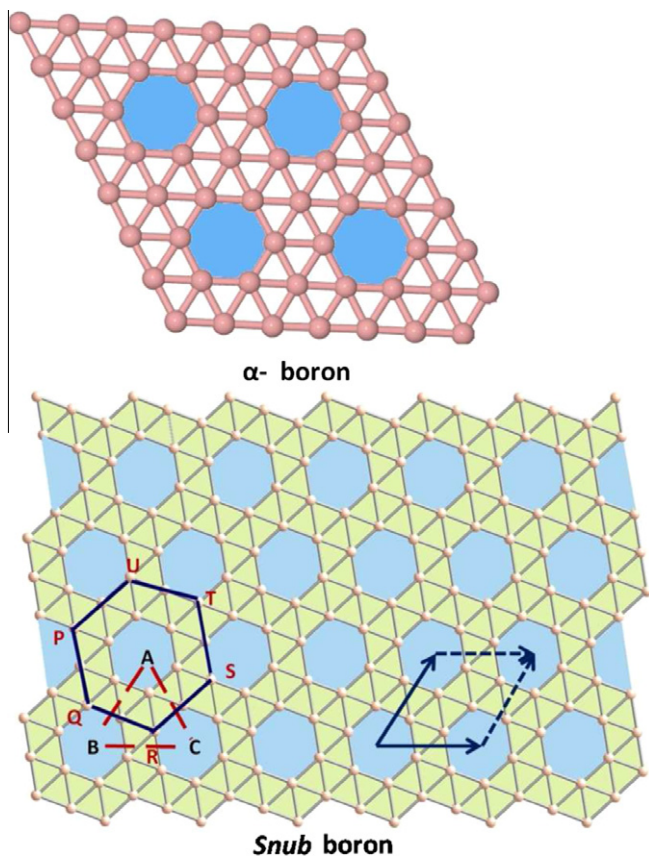


**Figure 2.** The  $\alpha$ -boron sheet (left) and the flat *snub* boron sheet compatible with the  $B_{60}$  fullerene (right).

of the perfectly symmetric icosahedral  $B_{60}$  is also known as *snub*-dodecahedron. Hence we call the related nanostructures (fullerenes, nanotubes, etc.) *snub*-nanostructures.

The *snub* boron sheet, like the  $\alpha$ -boron sheet has symmetrically distributed holes that are isolated from each other by triangular regions. However, unlike the  $\alpha$ -boron sheet in which the triangular regions are extended stripes, in the *snub* boron sheet these stripes are zigzag. The  $\alpha$ -boron sheet has two types of boron atoms: the boron atoms at the center of hexagonal rings with sixfold coordination and the boron atoms which are part of the hexagonal ring with fivefold coordination. In the *snub* boron sheet (and in related nanostructures), on the other hand, all boron atoms have five nearest neighbors. In this sense it is more symmetric than the  $\alpha$ -boron sheet. The hole density,  $\eta$ , for *snub* sheet is  $1/7$ , larger than the  $1/9$  of the  $\alpha$ -boron sheet. The calculations show that *snub* sheet is  $0.02$  eV/atom less stable than the  $\alpha$ -boron sheet. It may be possible to reduce the hole density by filling in some of the holes with boron atoms and gain some binding energy at the cost of loss of uniform fivefold coordination. We have not explored this in detail but a few such calculations did not show significant stabilization of the resultant sheets.

Larger *snub* boron fullerenes can be constructed by adding both the triangular and hexagonal rings to  $B_{60}$  in a such a way that the distribution of holes remains symmetric. Following the procedure for generating  $80n^2$  family of  $\alpha$ -boron sheet [18] we generate larger boron fullerenes. The procedure consists of cutting equilateral triangles from the planar sheet and pasting them on the faces of an icosahedron. The apices of the equilateral triangle have to be at the center of hexagons. Such an arrangement preserves the pattern of polygons in the sheet. Using such a procedure,  $60n^2$  family of chiral fullerenes containing triangles, hexagons and pentagons can be

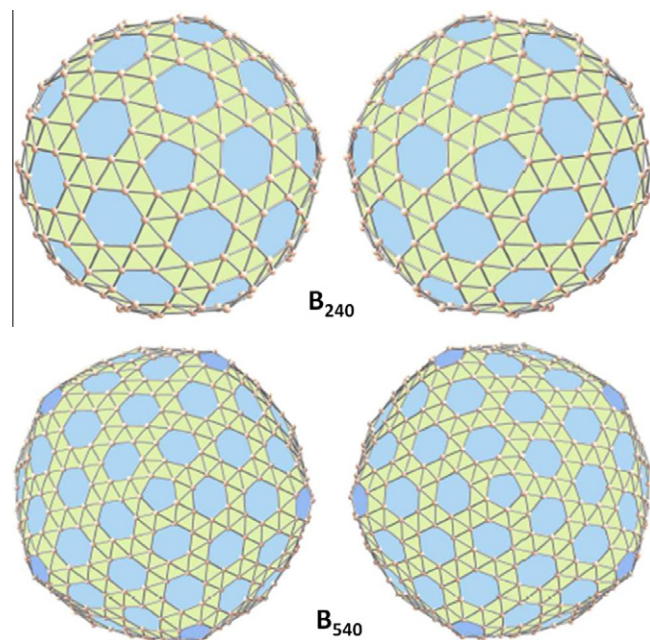


**Figure 3.** The  $B_{240}$  (top) and  $B_{540}$  (bottom) snub fullerenes. The structures on the right are the mirror images of the structures on the left.

constructed from the *snub* boron sheet. The first member of the family is  $B_{60}$ . The optimized geometries of the next two members ( $B_{240}$  and  $B_{540}$ ) are shown in Figure 3 and their binding energies are compared with other fullerenes in Table 1. To the best of our knowledge, this is the first time the structures of larger *snub* fullerenes are reported.

The Euler formula of polyhedra can be used to determine the number of atoms, triangles and hexagons in the *snub* boron fullerenes. If  $F$  is the number of faces (polygons),  $V$  is the number of vertices (atoms), and  $E$  is the number of edges then by Euler formula  $F + V = E + 2$ . The *snub* fullerenes have three different polygons: triangles, hexagons and pentagons. Each boron atom has fivefold coordination. If  $N_T$ ,  $N_H$ ,  $N_P$ ,  $N$  are number of triangles, hexagons, pentagons, and atoms, respectively, then using Euler formula it can be shown that  $N_T = 8N_H + 5N_P + 20$  and  $N = 6N_H + 4N_P + 12$ . The pentagons are holes and 12 pentagons are needed to form a closed structure. Thus, we have a general class of fullerenes with  $N = 6N_H + 60$ ;  $60n^2$  boron fullerene family being a subset of this class. For the smallest *snub* fullerene which has no hexagons Figure 1,  $N = 60$  and the number of triangles,  $N_T$  is 80. The number of holes in the general class is  $N_H + 12$  since each hexagon and the 12 pentagons have one hole each. The hole density,  $\eta$  would

**Table 1**

Binding energy (BE) of various boron sheets and fullerenes. The BE of  $\gamma B_{100}$  is estimated by adding the energy difference between the  $B_{80}$  and  $B_{100}$  from Ref. [22] to the present  $B_{80}$  binding energy.

System	Structure	BE (eV/atom)
Sheet	$\alpha$ -Boron	5.82
	<i>Snub</i> boron	5.80
	Triangular boron	5.51
	Hexagonal boron	4.94
Fullerene	<i>Snub</i> $B_{60}$	5.50
	<i>Snub</i> $B_{240}$	5.70
	<i>Snub</i> $B_{540}$	5.75
	$\alpha$ - $B_{80}$	5.64
	$\gamma$ - $B_{100}$	5.70

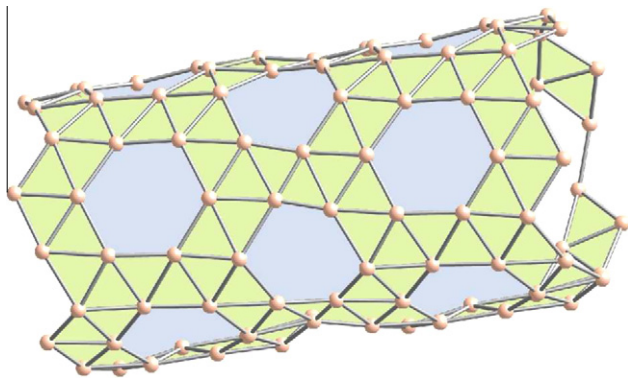


Figure 4. An infinite model of *snub* nanotube derived from the  $B_{60}$  fullerene.

be  $\frac{N_H+12}{7N_H+72}$ . Thus, in the asymptotic limit (as  $N \rightarrow \infty$ ), the  $\eta$  will approach  $1/7$  as it should, the hole density of *snub* boron sheet.

**Nanotubes:** The *snub* boron nanotubes can be constructed by simply rolling up the *snub* boron sheet. We have studied one such a nanotube which can be capped by hemispheres of the  $B_{60}$  fullerene. Its structure is shown in Figure 4. The binding energy of the infinite tube is 5.74 eV/atom and its band structure shows that tube is metallic. In view of recent report of boron nanotube synthesis [32] it will be interesting to further examine boron nanotubes of various diameters made from *snub* and other energetically competitive boron sheets.

In conclusion, using density functional calculations we illustrated an energetically stable novel family of chiral boron nanostructures. Starting from a *snub* icosahedral  $B_{60}$  fullerene which relaxes to a  $C_2$  structure, we obtained the compatible *snub* boron sheet which is only 0.02 eV/atom lower than the  $\alpha$ -boron sheet. The stability of the new boron sheet results from the symmetric distribution of the electron-rich and electron-deficient regions. The *snub* boron nanotube derived from  $B_{60}$  fullerene is metallic. The binding energies of the boron fullerenes and sheet are similar to that of the  $80n^2$  boron fullerenes and the related  $\alpha$ -boron sheet. Our preliminary work on metal coated boron nanostructures show that *snub* nanostructures can be more stable than  $\alpha$ -boron nanostructures. A recent work on Mg coated boron sheets also point to such energetic preference [33]. More work is required to explore such possibilities.

## Acknowledgement

The support for computational time at Texas Advanced Computing Center by the National Science Foundation through the TG-DMR090071 Grant is gratefully acknowledged.

## References

- [1] N.G. Szwacki, A. Sadrzadeh, B.I. Yakobson, Phys. Rev. Lett. 98 (2007) 166804.
- [2] N. Gonzalez Szwacki, Nanoscale Res. Lett. 3 (2008) 49.
- [3] K.C. Lau, R. Pandey, R. Pati, S.P. Karna, Appl. Phys. Lett. 88 (2006) 212111.
- [4] T. Baruah, M.R. Pederson, R.R. Zope, Phys. Rev. B 78 (2008) 045408.
- [5] A.K. Singh, A. Sadrzadeh, B.I. Yakobson, Nano Lett. 8 (2008) 1314.
- [6] D.L.V.K. Prasad, E.D. Jemmis, Phys. Rev. Lett. 100 (2008) 165504.
- [7] A.Y. Liu, R.R. Zope, M.R. Pederson, Phys. Rev. B (Condens. Matter Mater. Phys.) 78 (2008) 155422.
- [8] H. Tang, S. Ismail-Beigi, Phys. Rev. Lett. 99 (2007) 115501.
- [9] A. Ceulemans, J.T. Muya, G. Gopakumar, M.T. Nguyen, Chem. Phys. Lett. 461 (2008) 226.
- [10] K.C. Lau, R. Orlando, R. Pandey, J. Phys.: Condens. Matter 20 (2008) 125202 (10pp.).
- [11] H. He, R. Pandey, I. Boustani, S.P. Karna, J. Phys. Chem. C 114 (2010) 41494152.
- [12] A. Gindulyte, W.N. Lipscomb, L. Massa, Inorg. Chem. 37 (1998) 6544. PT: J.
- [13] A. Gindulyte, N. Krishnamachari, W.N. Lipscomb, L. Massa, Inorg. Chem. 37 (1998) 6546 (PT: J).
- [14] A.A. Quong, M.R. Pederson, J.Q. Broughton, Phys. Rev. B: Condens. Matter 50 (1994) 4787 (PUBM: Print publish).
- [15] I.J. Boustani, Solid State Chem. 133 (1997) 182.
- [16] I. Boustani, A. Quandt, EPL (Europhys. Lett.) 39 (1997) 527.
- [17] A. Quandt, I. Boustani, Chemphyschem 6 (2005) 2001.
- [18] R.R. Zope, T. Baruah, K.C. Lau, A.Y. Liu, M.R. Pederson, B.I. Dunlap, Phys. Rev. B: Condens. Matter Mater. Phys. 79 (2009) 161403(R).
- [19] Q.-B. Yan, X.-L. Sheng, Q.-R. Zheng, L.-Z. Zhang, G. Su, Phys. Rev. B: Condens. Matter Mater. Phys. 78 (2008) 201401.
- [20] R.R. Zope, EPL (Europhys. Lett.) 85 (2009) 68005 (6pp.).
- [21] R.R. Zope, T. Baruah, Phys. Rev. B 80 (2009) 033410.
- [22] C. Ozdoan, S. Mukhopadhyay, M. Hayami, Z. Gven, R. Pandey, I. Boustani, J. Phys. Chem. C 114 (2010) 43624375.
- [23] S. Mukhopadhyay, H. He, R. Pandey, Y.K. Yap, I.J. Boustani, Phys.: Conf. Ser. 117 (2009) 012028.
- [24] K.C. Lau, R.J. Pandey, Phys. Chem. C 111 (2007) 29062912.
- [25] L.C. Kinsey, T.E. Moore (Eds.), Symmetry, Shape and Space: An Introduction to Mathematics through Geometry, Wiley, John and Sons, Incorporated, 2001.
- [26] M.R. Pederson, B.M. Klein, J.Q. Broughton, Phys. Rev. B: Condens. Matter 38 (1988) 3825 (PUBM: Print publish).
- [27] K. Jackson, M.R. Pederson, Phys. Rev. B 42 (1990) 3276.
- [28] M.R. Pederson, K.A. Jackson, Phys. Rev. B 41 (1990) 7453.
- [29] G. Kresse, J. Furthmiller, Comput. Mat. Sci. 6 (1996) 15.
- [30] G. Kresse, D. Joubert, Phys. Rev. B 59 (1999) 1758.
- [31] D. Porezag, M.R. Pederson, Phys. Rev. A 60 (1999) 2840.
- [32] F. Liu, C. Shen, Z. Su, X. Ding, S. Deng, J. Chen, N. Xu, H. Gao, J. Mater. Chem. 20 (2010) 2197.
- [33] H. Tang, S. Ismail-Beigi, Phys. Rev. B 80 (2009) 134113.